PCCP

RSC Publishing

PAPER

View Article Online
View Journal | View Issue

Quantification of photocatalytic hydrogen evolution†

Cite this: *Phys. Chem. Chem. Phys.*, 2013, **15**, 3466

Michael Schwarze,*[a] Diana Stellmach,[b] Marc Schröder,[a] Kamalakannan Kailasam,[a] Rulle Reske,[a] Arne Thomas[a] and Reinhard Schomäcker[a]

Received 27th December 2012,
Accepted 17th January 2013

DOI: 10.1039/c3cp50168j

www.rsc.org/pccp

A new photoreactor with defined irradiation geometry was developed and tested for the water reduction reaction using carbon nitride (''C_3N_4'') as a photocatalyst. The hydrogen evolution rate was investigated with a sun simulator (I = 1000 W m^{-2}) in two different operation modes: circulation and stirring of the catalyst dispersion. Only in the stirred mode, where shear stress is lower, a stable hydrogen evolution rate of about 0.41 L m^{-2} h^{-1} is obtained. It is confirmed by experiments with D_2O that hydrogen is obtained from the water splitting process and not by dehydrogenation of the sacrificial agent. The obtained rate results in an efficiency of $<0.1\%$ based on a reference experiment with a photovoltaic-powered electrolysis setup. The change from distilled water to tap or simulated sea water results in a lower hydrogen evolution rate of about 50%.

1. Introduction

Hydrogen (H_2) is regarded as the energy carrier of the future because of its ''green'' energy-producing conversion and therefore efficient and sustainable H_2 production is of crucial importance. It is obvious that conventional hydrogen production *via* steam reforming of fossil fuels has to be replaced by greener and sustainable technologies due to diminishing fossil resources and emission of greenhouse gases. One approach is hydrogen production *via* electrolysis of water, with electrical energy obtained by energy transformation of renewables such as wind, water or sun.[1] The solar energy production (photovoltaic) is already well investigated and the efficiency can reach values up to 25%.[2] Efficiency for low temperature electrolysis is in the order of 75%,[3] so that for photo-voltaic powered electrolysis an overall efficiency of 19% is possible (16% was already reported by Wang *et al.*[4]). A further attempt for green hydrogen production is photocatalytic water splitting which has become a dream reaction since Fujishima and Honda have made their first successful observations on TiO_2 electrodes in 1972.[5] Whereas in photovoltaic-powered electrolysis the total efficiency depends on the single energy transformation steps, in photocatalysis the efficiency is a characteristic property of the chosen photocatalyst, which can be a homogeneous catalyst complex or a heterogeneous semiconductor, and its feature to make use of the absorbed light. With respect to a technical application heterogeneous catalysts are favorable, but up to now there are only a few heterogeneous systems that are able to perform overall water splitting with a single photocatalyst or with two photocatalysts.[6,7] To find suitable photocatalysts that can be combined for overall water splitting and to investigate structure–activity relationships, the individual half reactions are often studied. To study the half reactions, a sacrificial agent is added to water that acts as an electron donor (H_2 evolution) or an electron acceptor (O_2 evolution), respectively. In recent years mostly inorganic semiconductors were used in UV and visible light irradiation such as metal oxides, metal nitrides, sulfides, oxynitrides, and oxysulfides.[7] Recently, metal-free, polymeric graphitic carbon nitrides as organic semiconductors were explored for the evolution of H_2 and O_2 using visible light.[8] While the bulk polymeric carbon nitrides show lower hydrogen evolution rates, it has been shown that modifying the chemical structure or nanostructure of the materials can largely increase their photocatalytic efficiency. For example porous structures with high surface area were produced which enhance the catalytic performance of the carbon nitrides to a large extent. Hard templating approaches can be applied to create porosity in these materials, *e.g.* silica and alumina.[9–14] Herein, a recently developed sol–gel/thermal condensation route was employed to synthesize continuous mesoporous structures of carbon nitrides.[15]

In general, a comparison of published results regarding photocatalytic efficiency of many photocatalysts for H_2 or O_2 evolution is often impossible due to completely different reaction conditions or test reactors. To perform photocatalytic hydrogen evolution reactions with UV or visible light irradiation using homogenous or heterogeneous photocatalysts, three types of

[a] *Technische Universität Berlin, Department of Chemistry, Straße des 17. Juni 124, 10623 Berlin, Germany. E-mail: ms@chem.tu-berlin.de*

[b] *Helmholtz Zentrum Berlin, Hahn-Meitner-Platz 1, 14109 Berlin, Germany*

† Electronic supplementary information (ESI) available. See DOI: 10.1039/c3cp50168j

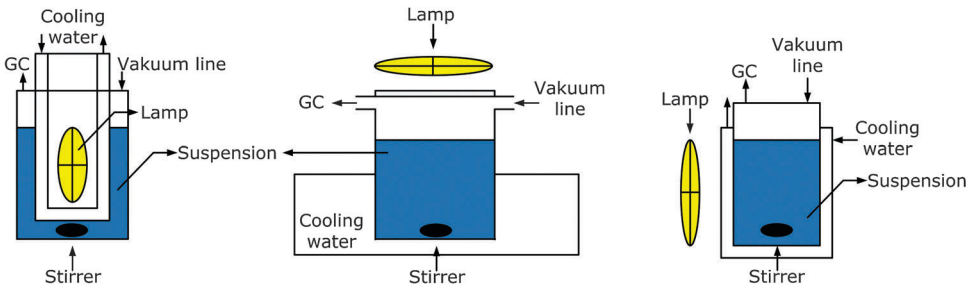

Fig. 1 Scheme of typical test reactors for photocatalytic reactions (left: inner irradiation, middle: top irradiation, right: side irradiation).

photo reactors are commonly used: reactors with (a) inner irradiation,[16] (b) top irradiation,[17,18] and (c) side irradiation[19] (Fig. 1).

In this contribution, we introduce a photoreactor that allows for quantitative investigation of photocatalysis, due to defined irradiation geometry. Reactor performance is studied with the hydrogen evolution reaction using sol–gel prepared carbon nitride as a photocatalyst. Using this optimized setup, we also investigated the stability of the photocatalyst and the influence of water quality on the photocatalytic activity of polymeric carbon nitrides. Furthermore hydrogen evolution rates are compared to photovoltaic powered electrolysis to evaluate the efficiency.

2. Experimental part

2.1 Chemicals

For photocatalytic hydrogen evolution, mesoporous carbon nitride was used as a photocatalyst (see Section 2.2), chloroplatinic acid solution (8 wt%, Sigma-Aldrich) or chloroplatinic acid (≥37.5% Pt basis, Sigma-Aldrich) was used as a precursor for platinum, used as a co-catalyst, distilled water was used as a hydrogen source, and triethanolamine (TEOA, ≥99% purity, Sigma-Aldrich) was used as a sacrificial agent. Deuterium oxide (D_2O, 100%, Roth) was used in one experiment to study the origin of hydrogen evolution. In electrolysis experiments, sulfuric acid (≥95%, Roth) was added to increase water conductivity.

2.2 Photocatalyst

Mesoporous graphitic carbon nitride, mpg-SG-CN-6, was prepared using a published procedure.[15] Cyanamide (CA) used as a carbon nitride precursor was mixed with tetraethylorthosilicate (TEOS), used as the silica template (1 : 6 molar ratios of TEOS : CA). After aging at 80 °C, the composites are thermally treated at 550 °C to obtain the carbon nitride–silica composites. Finally carbon nitride, mpg-SG-CN-6 (abbreviated as CN6), is obtained by the removal of silica using NH_4HF_2 solution.

The structural identity of this mesoporous carbon nitride was verified by XRD, UV-Vis spectroscopy and BET measurements (see ESI†). The surface area of CN6 in this work is about 173 $m^2\ g^{-1}$, pore diameter is about 40 Å, and total pore volume is about 0.28 $cm^3\ g^{-1}$. The activity of the photocatalyst was already investigated by Kailasam *et al.*[15] and the mean rate using a Xe-lamp (395 nm cut-off filter, I = 15 000 W m^{-2}, 25 °C) in combination with a side irradiated batch reactor is ~1.7 mL h^{-1}.

2.3 Photocatalytic reactions

Photocatalytic experiments were performed using two different operation modes. In mode 1, the reaction solution was circulated by a gear pump (BVP-Z, Ismatec, Germany) between the reservoir and the photoreactor, both connected to a thermostat (Eco Gold, Lauda DR. R. WOBSER GmbH & Co. KG). The solution in the reservoir was stirred to avoid catalyst settlement. In mode 2, the reaction solution was stirred within the photoreactor connected to the thermostat. In each case, a thermocouple was used to control the reaction temperature. The scheme for both operation modes is shown in Fig. 2.

For the photocatalytic experiments a newly designed photoreactor which is shown in Fig. 3 was used. The photoreactor was modularly designed to allow for two different operation modes.

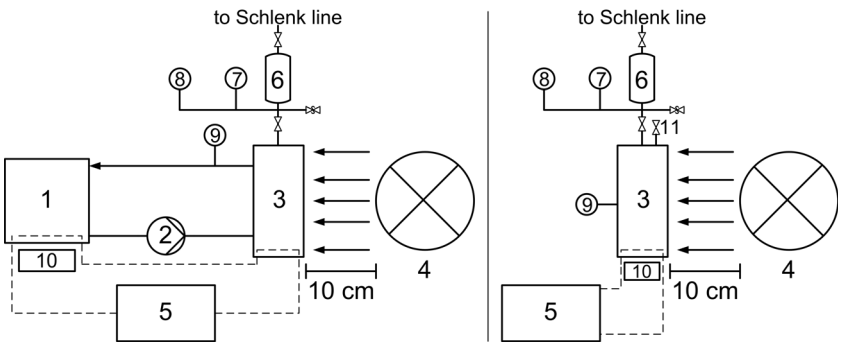

Fig. 2 Scheme of the setup used for photocatalytic experiments (mode 1 is shown left and mode 2 right): (1) reservoir, (2) delivery pump, (3) photoreactor, (4) lamp, (5) thermostat, (6) gas tank, (7) manometer, (8) pressure sensor, (9) thermocouple, (10) magnetic stirrer, and (11) dosing valve.

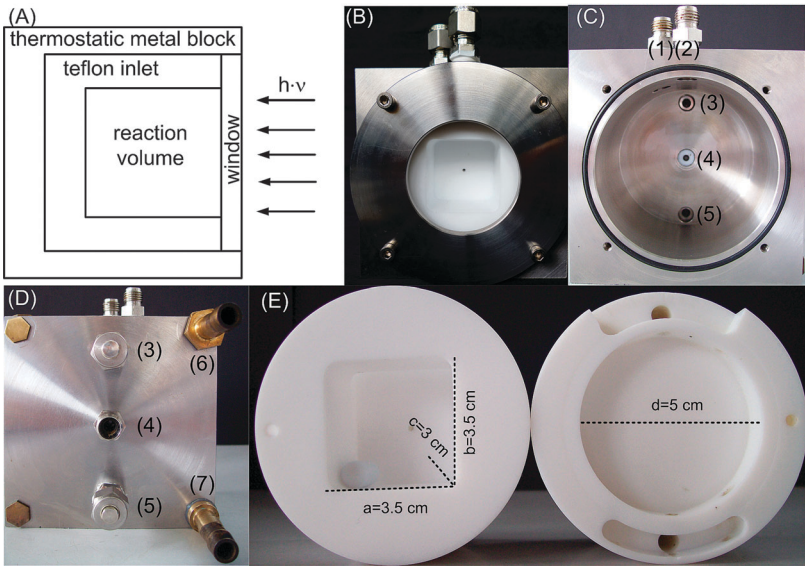

Fig. 3 Reactor for photocatalytic hydrogen evolution: (A) scheme of the photoreactor, (B) front view of the photoreactor, (C) front view of the metal block (D) back view and (C) inlets for irradiation with stirred (left) and circulated (right) reaction solution. In experiments with stirred solution, the reactor is charged with the liquids at position (1) and the thermocouple is placed at position (4). In experiments with circulated solution, the stream enters and leaves the reactor at position (5) and (3), respectively. Reactor is connected to the pressure sensor over position (2) and to a thermostat over position (6) and (7), respectively.

The photoreactor window was made from quartz glass (Aachener Quarz-Glas Technologie Heinrich, Germany) with a thickness of 6 mm. For the experiments, two different lamps were tested: a 300 W Xe arc lamp and a sun simulator. The light intensity was adjusted to 1.5 W cm^{-2} (Xe lamp, water filter was used) and 1000 W m^{-2} (sun simulator) using a thermopile. Lamps and thermopile were received from L.O.T.-Oriel GmbH & Co. KG.

The top of the photoreactor (see ESI†) was connected to a gas line equipped with a manometer (Kobold Messring GmbH, Germany), a gas tank (V = 150 mL, B.E.S.T. Fluidsysteme GmbH, Germany,), and a pressure sensor (Type-P30, ΔP = ±0.1%, WIKA Alexander Wiegand SE & Co. KG, Germany) to monitor the pressure increase due to hydrogen evolution. To work under inert conditions, a Schlenk line with argon as an inert gas was connected to the setup over the gas tank.

In a standard mode 1 experiment, 100 mg mpg-SG-CN6 was placed in the reservoir and then 50 mL of an aqueous TEOA solution (10 vol% TEOA) containing the platinum precursor (10 wt% H_2PtCl_6) was added. After closing the reservoir, the stirrer was turned on to avoid particle segregation within the reservoir (300–400 rpm) and the headspace was evacuated and refilled with argon up to five times. The delivery pump, to circulate the catalyst dispersion between the reservoir and the photoreactor, and the thermostat were started (T = 25 °C). When the reaction temperature was reached, the lamp was switched on and the computer program started to record temperature and pressure.

In a standard mode 2 experiment, 50 mg mpg-SG-CN6 was placed in the photoreactor (located on a magnetic stirrer) and the photoreactor was evacuated and refilled with argon up to five times. Then 38 mL of aqueous TEOA solution (10 vol% TEOA) containing the platinum precursor (10 wt% H_2PtCl_6) was added under an argon flow. The stirrer, to rotate a magnetic stirrer bar placed within the photoreactor itself, and the thermostat were started (T = 25 °C). The residual steps are similar to mode 1.

H_2O and TEOA were pretreated before use. H_2O was firstly degassed for 1 h under vacuum in an ultrasonic bath and secondly purged with argon for 1 h. TEOA was purged for 1 h with argon. After the reaction, a sample of the headspace was analyzed with GC for hydrogen content.

2.4 Photovoltaic-powered electrolysis

Electrolysis was carried out in a Hoffman Electrolizer (Conatex Didactic GmbH, Germany) with diluted sulfuric acid (20 vol%) as an electrolyte. The electrodes were shiny platinum sheets ($A_{electrode}$ = 1.4 cm^2). To generate the power for electrolysis experiments, a 10 × 10 cm^2 thin film solar module (10 cells, 650 mV each cell) was completely irradiated using the same lamps as in the photocatalytic experiments. The solar cell consists of copper indium disulfide (CIS) as a p-type semiconductor, zinc oxide (ZnO) as an n-type semiconductor, and cadmiumsulfide (CdS) as a buffer layer.

The efficiency of photovoltaic-powered electrolysis (η_{pvpe}) was calculated from eqn (1).

$$\eta_{pvpe} = \eta_{sm}\eta_{we} \quad (1)$$

In eqn (1), η_{sm} is the efficiency of the solar module and η_{we} is the efficiency of the Hoffman Electrolizer. The efficiency of the solar module was calculated from eqn (2).

$$\eta_{sm} = \frac{I_{MPP}U_{MPP}}{E_L A} \quad (2)$$

In eqn (2), I_{MPP} is the currency at the maximum power point, U_{MPP} is the voltage at the maximum power point, E_L is the irradiation intensity, and A is the area of the solar module (100 cm^2).

The efficiency of the Hoffman Electrolizer (η_{we}) was calculated from eqn (3).

$$\eta_{we} = \eta_f \eta_{en}$$
$$\eta_f = \frac{V(H_2)_{ex}}{V(H_2)_{theo}} = \frac{zFV(H_2)_{ex}}{ItV_m} \quad (3)$$
$$\eta_{en} = \frac{\Delta_R H}{zFU}$$

In eqn (3), η_f is the Faraday efficiency, η_{en} is the energetic efficiency, z is the number of transferred electrons (z = 2 for 1 mol hydrogen), F is the Faraday constant, $V(H_2)_{ex}$ is the hydrogen volume obtained in electrolysis, I is the applied current, t is the time for which constant current was applied, V_m is the molar volume of hydrogen, $\Delta_R H$ is the reaction enthalpy (285.9 kJ mol^{-1} for liquid water), and U is the applied voltage.

2.5 Characterization

An Agilent 7890A gas chromatograph was used to determine the hydrogen content in the headspace. The GC was equipped with a carboxen-1000 column and a thermal conductivity detector (TCD). The carrier gas was argon (30 mL min^{-1}). Nitrogen sorption analyses were carried out on an Autosorb-1 instrument after evacuating the samples at 150 °C overnight. The surface areas are determined by applying the Brunauer–Emmett–Teller (BET) method in a relative pressure range of 0.05–0.25. The pore volume is calculated at a relative pressure of 0.99. An OmniStar GSD 301C quadrupole mass spectrometer from Pfeiffer Vacuum equipped with a tungsten filament was used to detect the different hydrogen species (H_2, HD, and D_2) in experiments with isotopic labeled water. The voltage of the secondary electron multiplier (SEM) was 1050 V.

3. Results and discussion

3.1 Development and operation of the photoreactor

The main focus of this contribution was the development of a defined photoreactor that can be used to quantitatively study photocatalytic hydrogen evolution. It is obvious that the photocatalyst must absorb light to generate hydrogen from water; therefore, a defined light injection into the photoreactor is important. Here, the photoreactor is equipped with a side-placed planar quartz glass window in analogy to a photometer cuvette. The loss in light intensity is less than 5% for wavelengths higher than 250 nm, because of the perpendicular irradiation of the glass window. This fact was proven by absorption experiments in an UV/Vis spectrometer. But it should be mentioned that material deposition on the inner side of the glass window during the photocatalytic experiment can influence the reaction rate. The advantages of using a planar window are that no light is scattered like in conventional reaction vessels and that the area used for irradiation is exactly known, so it can be used to calculate an area-based reaction rate (see Section 3.2). The connections between the single parts of the setup were made of stainless steel to avoid gas losses during the photocatalytic experiments. The typical leakage rate was about 1 mbar h^{-1}. To follow the reaction, we used a simple pressure measurement. If only hydrogen is produced during the reaction, the amount of evolved hydrogen is given by the pressure and can be calculated from the ideal gas law (eqn (4)).

$$V(H_2) = V_m n(H_2) = V_m \frac{p(V_{total} - V_{liquid})}{RT} \quad (4)$$

In eqn (4), V_m is the molar volume of hydrogen, $n(H_2)$ is the obtained moles of hydrogen, p is the pressure, R is the ideal gas constant, T is the reaction temperature, V_{total} is the total volume of the setup, and V_{liquid} is the volume of the reaction solution. It is known that hydrogen solubility in water is very low; therefore, it was neglected in our calculations. GC analysis was used to detect the amount of hydrogen in the gas phase after reaction and the results of GC analysis and pressure measurement agree well. Based on the used quartz glass window with a thickness of 6 mm and a total visible area of 19.6 cm^2, the maximum allowed pressure difference for safe work was 2 bar. In the case of higher catalytic activity which will lead to a fast pressure increase, a gas tank was installed as additional volume. The gas tank also serves as a hydrogen storage vessel, so that the produced hydrogen can be used in other applications. Furthermore, it is possible to connect the setup directly to other applications, *e.g.* a fuel cell.

3.1.1 Performance of photocatalytic H_2 evolution in different operation modes. If a heterogeneous photocatalyst is dispersed in an aqueous-solution, it will settle down with time depending on the characteristics of the solid, *i.e.* its dispersibility. For two CN6 dispersions with different concentrations we measured the light absorption with time to investigate the settling process and after one hour the relative absorption was about 50%. This means, a bigger part of the photocatalyst that would be unable to utilize light in a photocatalytic experiment has settled down. To avoid settling during the photocatalytic experiments, two operation modes as explained in the experimental part were used: one with circulation of the catalyst dispersion and one with stirring of the catalyst dispersion. The H_2 evolution profiles are shown in Fig. 4.

In the case of the circulated dispersions, acceptable hydrogen evolution is only obtained at moderate flow rates. If the flow rate is low, shear stress is low but some of the particles may still settle down. At higher flow rates probability for particle deposition decreases, but shear stress increases and can damage the photocatalyst. As a result, the particle diameter decreases and a higher number of grain boundaries are obtained which might assist the recombination of the formed electron–hole pair leading to a decreased H_2 evolution rate. The change in particle size as a function of the flow rate was investigated by SEM from CN6 samples dispersed only in water and circulated (Fig. 5). It is obvious that at high flow rates the assumed small particles are produced. It should be noted that, to the best of our knowledge, so far no works have been published regarding the influence of particle size or morphology of polymeric carbon nitrides on the observed hydrogen evolution rate (HER). As shown in this experiment, actually simple grinding can largely change the observed HER; thus the mean particle size

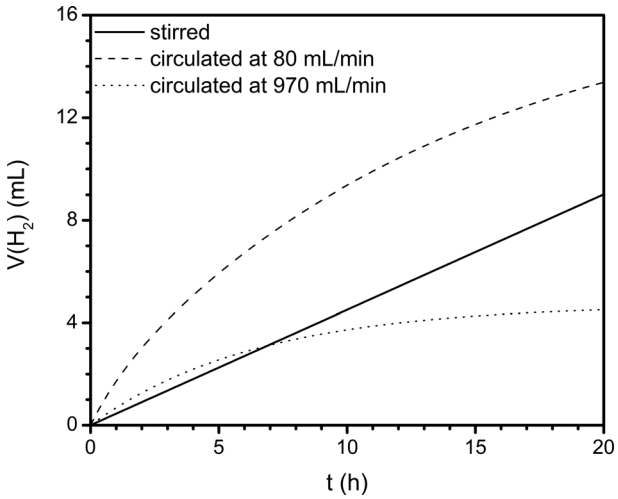

Fig. 4 Evolved H_2 volume for circulated and stirred CN6 dispersions measured with a sun simulator (5 wt% H_2PtCl_6, 10 vol% TEOA, 25 °C).

of this photocatalyst cannot be neglected when discussing its photocatalytic activity and might even be the actual reason for changes in the photocatalytic activity when novel synthetic protocols are introduced to modify polymeric carbon nitrides.

For the stirred dispersion, the shear stress is much lower and a constant activity is obtained. The appearance of the photocatalyst after reaction on the same time scale shows no change in the particle size (Fig. 6), but a long-term experiment (t > 1 month) resulted also in smaller particles.

Besides the structure of the photocatalyst the formation of the active species also has to be considered. In our case, we added H_2PtCl_6 as a co-catalyst precursor that forms Pt nanoparticles during irradiation which will deposit on CN6. This "*in situ*" co-catalyst preparation is a typical procedure often described in the literature. As generally known from heterogeneous catalysis, the formation of supported nanocatalysts is not an easy task. In general, the size of the nanoparticles and

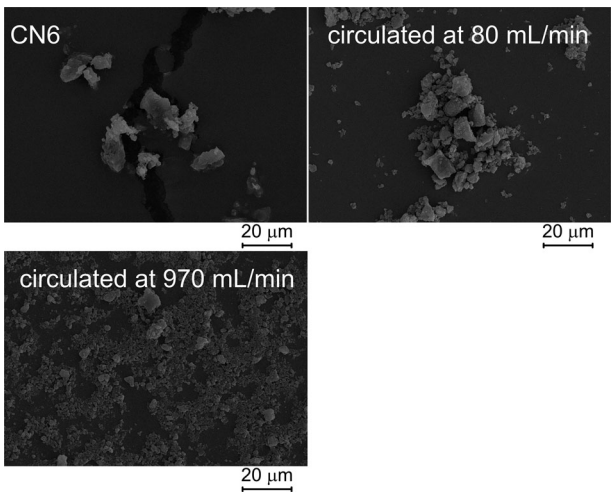

Fig. 5 SEM pictures of the photocatalyst before (upper left), after circulation at 80 mL min^{-1} (upper right) and after circulation at 970 mL min^{-1} (lower left).

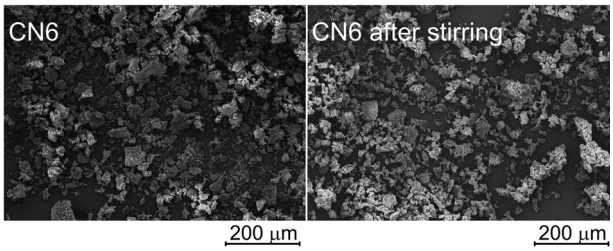

Fig. 6 SEM pictures of the photocatalyst before (left) and after photocatalytic experiment with stirred catalyst dispersion (right).

the dispersion on the support have an impact on the catalytic activity. We assume that the deposition process is less controlled when the dispersion is circulated. In our experiments the highest activity was found for 10 wt% H_2PtCl_6 with respect to the photocatalyst mass. Based on our observations and obtained hydrogen profiles, the stirred system is favored for kinetic investigations.

To identify the origin of the evolved hydrogen, a photocatalytic experiment with isotopically labeled water (composition: H_2O, D_2O and TEOA) was carried out. It is possible that hydrogen is released from the photocatalyst as a residue from the synthesis process, but the identification of D_2 and HD *via* MS is a proof that during the photocatalytic experiment H_2 is obtained from water splitting. Two cases can be discussed this way: H_2 is released from water or by dehydrogenation of the alcohol used as a sacrificial agent. To find an answer for this discussion, a second experiment was performed with a mixture of D_2O (85 vol%) and TEOA (15 vol%) only. The mass spectrometry analysis resulted in a mixture of 85.4% D_2, 12.9% HD, and 1.7% H_2. The high fraction of D_2 is a proof for hydrogen obtained by water splitting but the presence of HD also indicates H–D exchange between D_2O and TEOA.

3.1.2 Influence of water quality. Many photocatalytic experiments are carried out using very pure water (millipore or distilled water), but to avoid water purification steps prior to photocatalysis the photocatalyst should accept water of any quality. Here, we investigated the influence of the water quality on the hydrogen evolution rate with a sacrificial agent and the highest rates are obtained for millipore and distilled water as shown in Fig. 7. However, if tap water or simulated sea-water is used the rate decreases by about 50%. We assume that at higher ion strengths parallel reactions occur where the photogenerated electrons are consumed by the ions. That means, if there is a highly active and stable photocatalyst, it should be possible to apply a process for large scale hydrogen production using conventional water supply.

3.1.3 Stability tests. To complete our investigations regarding the setup, we simulated different malfunctions (Fig. 8). At first, we tested the influence of light loss in light on–light off experiments. This is representative for a day–night cycle, and for photovoltaic-powered electrolysis it is known that fluctuations in the intensity/amperage can lead to corrosion of electrodes. We could clearly identify that no hydrogen is produced in the absence of light and after light is turned on again, the rate is re-established.

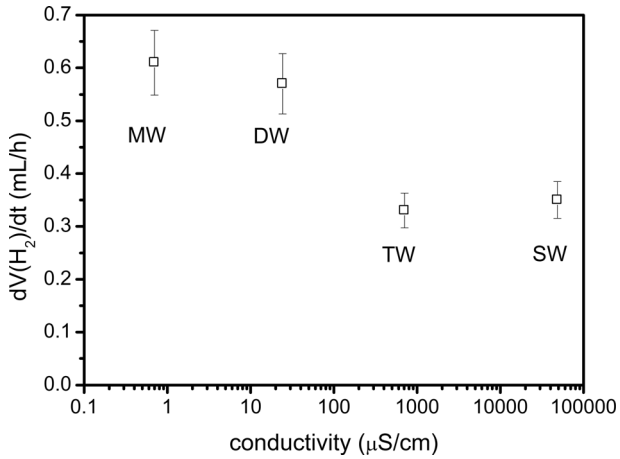

Fig. 7 Hydrogen evolution rates (10 wt% H_2PtCl_6, 10 vol% TEOA, 25 °C) for water of different quality (MW: millipore water, DW: distilled water, TW: tap water, SW: simulated sea-water (5 wt% NaCl)).

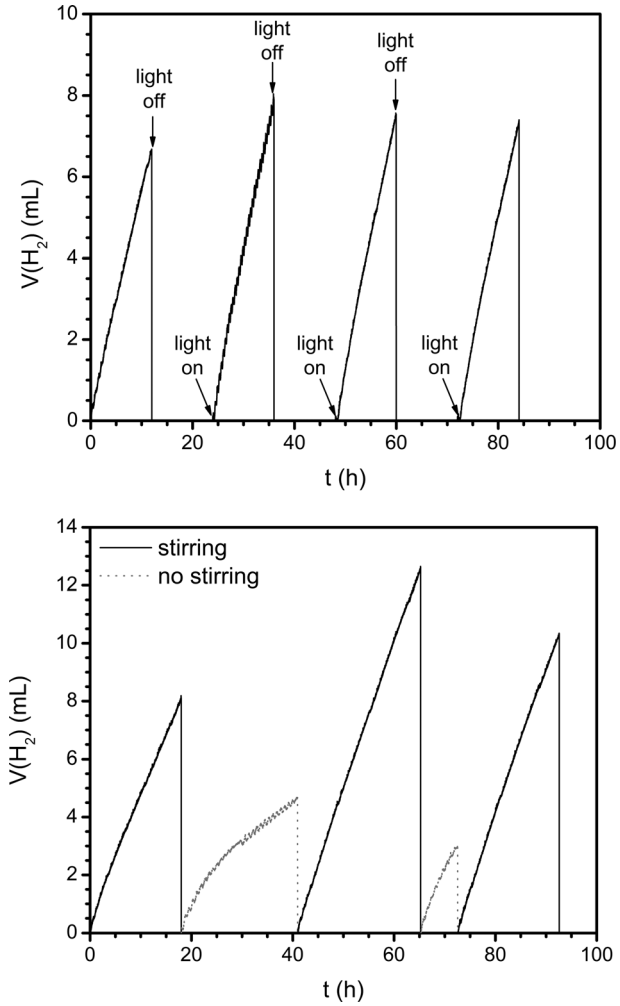

Fig. 8 Simulation of malfunctions: light breakdown (top) and no stirring (bottom).

Thereafter, we tested a stirrer breakdown. When the stirring rate is set to zero, the particles begin to settle (as already mentioned) and the rate decreases. The main question is the re-dispersibility of the catalyst. After restarting the stirrer, the particles are immediately re-dispersed and also in this case the rate is re-established. Based on these two tests we assume that the catalyst is stable under the chosen conditions.

3.2 Reaction rate

When the rate of hydrogen evolution is calculated, commonly μmol h^{-1} and mL h^{-1} are used as units. For a better comparison of the results that come from different setups, a reference is needed. Because heterogeneous catalysts are used in many photocatalytic experiments, the amount of photocatalyst seems to be a good reference. But photocatalytic activity is not linearly correlated to the photocatalyst concentration and above a ''limiting'' concentration the rate will become constant; therefore, a better reference is needed. With respect to photovoltaic, the area of irradiation seems to be appropriate because the area can largely differ between different photocatalytic setups even if the photocatalyst concentration is above the ''limiting concentration''. Therefore, the unit for the rate of hydrogen evolution should be mol m^{-2} h^{-1} or L m^{-2} h^{-1}. For some catalysts investigated with a sun simulator where the area of the irradiation window is mentioned in the experimental part, the area-based H_2 evolution rate was calculated (see Table 1). Due to the different setups, the rates given in μmol h^{-1} largely differ and it seems that among the selected photocatalysts CdS is the best. In comparison to CN6 its rate looks 300 times higher, but after recalculation under consideration of the irradiation area, all rates are much closer to each other and the ratio of CdS/CN6 is only 18.

If a Xe arc lamp is used as a light source, the hydrogen evolution rate increases by a factor of 2–3 because of a much higher light intensity even if a UV-light cut-off filter is used. Many research groups only mention the lamp but miss to give additional information, *e.g.* which light intensity is used and how was the lamp calibrated. Therefore, it is very difficult to compare rates which are obtained using other lamps than a sun simulator whose intensity is typically fixed to a value of 1000 W m^{-2}.

3.3 Efficiency of photocatalysis

To assess the efficiency of hydrogen production in the photocatalytic experiments, it is necessary to have a reference system. Here, a photovoltaic-powered electrolysis setup was used to generate hydrogen from water with the same light source as in

Table 1 Area-based hydrogen evolution rates for different photocatalysts measured with a sun simulator

Entry	Photocatalyst	Co-catalyst	Rate (μmol h^{-1})	Rate (mol m^{-2} h^{-1})	Ref.
1	$Ba_5Ta_4O_{15-x}N_x$	Pt	495	0.20	20
3	CN6	Pt	20	0.02	—
4	CdS	Pd/Cr_2O_3	6122	0.35	21
5	$ZnS–AgInS_2–CuInS_2$	Ru	1150	0.35	22
6	Ag_2S/CdS	Pt	85	—	23

Table 2 Efficiency of photovoltaic-powered electrolysis

Light source	$dV(H_2)/dt$ (mL h^{-1})	η_f (%)	η_{en} (%)	η_{sm} (%)	η_{pvpe} (%)
300 W Xe arc lamp	8.4	87.5	57.3	2.1	1.0
Sun simulator	8.2	94.0	49.2	3.3	1.5

the photocatalytic experiments. The efficiency for the used lamps is given in Table 2.

The efficiency of the chosen test cell was 2.1% for the Xe lamp and 3.3% for the sun simulator. These low values were caused by the small dimensions of this cell that was adjusted to the experimental setup. For CN6, the hydrogen production rate is about 0.5 mL h^{-1} for the sun simulator, while in photovoltaic-powered electrolysis the rate is 8.2 mL h^{-1} for the same lamp. Based on the calculated efficiency for the electrolysis system, which is 1.5%, the efficiency of the photocatalytic experiment (η_{PC}) is easily obtained by comparison of the hydrogen evolution rates as shown in eqn (5)

$$\eta_{PC} = \frac{HER_{PC}}{HER_{PVPE}}\eta_{PVPE} = \frac{HER_{PC}}{8.2\ mL\ h^{-1}}1.5\% \qquad (5)$$

For the CN6 photocatalyst under the chosen reaction conditions, the efficiency is 0.09%. As already mentioned in the introduction, the efficiency for photovoltaic-powered electrolysis can reach values between 15–25% and to be competitive, the efficiency of photocatalytic hydrogen evolution with CN6 as photocatalyst must be increased. If we aim for an efficiency of 15% then the activity of the photocatalyst should increase by a factor of about 160. Considering the significant developments in photocatalytic activities which have been reached in the recent years by modifying the structure of the initially used bulk polymeric carbon nitrides, further modifications may lead to higher activities. At this point it is not possible to say whether the needed efficiency can be achieved with a carbon nitride material, but as shown in Table 1, there are already photocatalysts with significantly higher activity so that one day photocatalysis can be a real alternative for hydrogen production.

4. Summary

A photoreactor with defined irradiation geometry was developed that can be used for continuous and batch photocatalytic experiments. The setup was tested with carbon nitride as a photocatalyst and while the catalyst was subjected to strong shear stress in continuous experiments, the catalyst stayed stable in batch experiments. The hydrogen evolution rate for the photocatalyst with *in situ* Pt loading and triethanolamine as a hole scavenger is about 0.5 mL h^{-1} or, with the irradiation area as a reference, 0.41 L m^{-2} h^{-1}. The catalyst shows the same activity after different interruptions, *e.g.* light off or no stirring. It is confirmed from experiments with D_2O that hydrogen is obtained from water splitting and not by dehydrogenation of the sacrificial agent. If tap or simulated sea water is used, the hydrogen evolution rate is about 50% lower than for distilled water. To access the efficiency of the photocatalyst, the hydrogen evolution rate of the photocatalyst was compared with the rate obtained for photovoltaic-powered electrolysis. The efficiency is 0.09% and needs further improvement (at least by a factor of 100) to be competitive.

Acknowledgements

This work was supported by the BMBF (Spitzenforschung und Innovation in den neuen Ländern, FKZ 03IS2071D).

References

1 T. Abbasi and S. A. Abbasi, *Renewable Sustainable Energy Rev.*, 2011, **15**, 3034–3040.
2 V. Avrutin, N. Izyumskaya and H. Morkoç, *Superlattices Microstruct.*, 2011, **49**, 337–364.
3 M. A. Laguna-Bercero, *J. Power Sources*, 2012, **203**, 4–16.
4 Z. Wang, R. R. Roberts, G. F. Naterer and K. S. Gabriel, *Int. J. Hydrogen Energy*, 2012, **37**, 16287–16301.
5 A. Fujishima and K. Honda, *Nature*, 1972, **238**, 37–38.
6 K. Maeda, *J. Photochem. Photobiol., C*, 2011, **12**, 237–268.
7 A. Kudo and Y. Miseki, *Chem. Soc. Rev.*, 2009, **38**, 253–278.
8 X. Wang, K. Maeda, A. Thomas, K. Takanabe, G. Xin, J. M. Carlsson, K. Domen and M. Antonietti, *Nat. Mater.*, 2009, **8**, 76–80.
9 K. Maeda, X. Wang, Y. Nishihara, D. Lu, M. Antonietti and K. Domen, *J. Phys. Chem. C*, 2009, **113**, 4940–4947.
10 X. Wang, K. Maeda, X. Chen, K. Takanabe, K. Domen, Y. Hou, X. Fu and M. Antonietti, *J. Am. Chem. Soc.*, 2009, **131**, 1680–1681.
11 X. Chen, Y.-S. Jun, K. Takanabe, K. Maeda, K. Domen, X. Fu, M. Antonietti and X. Wang, *Chem. Mater.*, 2009, **21**, 4093–4095.
12 A. Thomas, *Angew. Chem., Int. Ed.*, 2010, **49**, 8328–8344.
13 A. Thomas, F. Goettmann and M. Antonietti, *Chem. Mater.*, 2008, **20**, 738–755.
14 Y.-S. Jun, W. H. Hong, M. Antonietti and A. Thomas, *Adv. Mater.*, 2009, **21**, 4270–4274.
15 K. Kailasam, J. D. Epping, A. Thomas, S. Losse and H. Junge, *Energy Environ. Sci.*, 2011, **4**, 4668.
16 Z. Zou, J. Ye, K. Sayama and H. Arakawa, *J. Photochem. Photobiol., A*, 2002, **148**, 65–69.
17 H. W. Kang and S. Bin Park, *Int. J. Hydrogen Energy*, 2011, **36**, 9496–9504.
18 K. Maeda, H. Terashima, K. Kase and K. Domen, *Appl. Catal., A*, 2009, **357**, 206–212.
19 F. Gärtner, A. Boddien, E. Barsch, K. Fumino, S. Losse, H. Junge, D. Hollmann, A. Brückner, R. Ludwig and M. Beller, *Chem.–Eur. J.*, 2011, **17**, 6425–6436.
20 A. Mukherji, C. Sun, S. C. Smith, G. Q. Lu and L. Wang, *J. Phys. Chem. C*, 2011, **115**, 15674–15678.
21 W. Yao, C. Huang, N. Muradov and A. T. Raissi, *Int. J. Hydrogen Energy*, 2011, **36**, 4710–4715.
22 I. Tsuji, H. Kato and A. Kudo, *Angew. Chem., Int. Ed.*, 2005, **44**, 3565–3568.
23 S. Shen, L. Guo, X. Chen, F. Ren and S. S. Mao, *Int. J. Hydrogen Energy*, 2010, **35**, 7110–7115.

